JOURNAL OF MATERIALS SCIENCE 32 (1997) 3571–3575

Preparation of nanoscale iron and Fe_3O_4 powders in a polymer matrix

LEI CHEN, WENG-JUN YANG, CHANG-ZHENG YANG
Institute of Chemistry and Chemical Engineering, Nanjing 210093, Peoples Republic of China

The synthesis of the title matrix-mediated nanocomposite was performed in both poly(4-vinylpyridine) homopolymer and vinylstyrene-4-vinylpyridine copolymers. NH_2–NH_2 was used as the reducing agent to prepare the polymer-supported metallic particles which were later converted into fine oxide powders by oxidation. The structure and morphology of the products were studied by Fourier transform infrared spectroscopy, wide angle X-ray diffraction, transmission electron microscopy as well as electron spectroscopy for chemical analysis and magnetic measurements. The wide angle X-ray diffraction patterns contained reflections that could be assigned to Fe_3O_4 particles while no reflections were observed that correspond to ultrafine iron powders. The magnetization behaviour of the nanocomposite was determined by the degree of loading of Fe in the polymer matrix.

1. Introduction

Interest in condensed matter at size scales larger than that of atoms but smaller than that of bulk solids has rapidly grown over the past two decades. This matter containing only tens to thousands of atoms can have structures and properties quite different from those of conventional materials. A variety of methods to grow these nanostructures have been applied and these include molecular beam epitaxy, chemical vapour deposition and gas condensation. The synthesis of materials by the consolidation of small clusters was first suggested in the early 1980s [1] and was applied initially to metals and then to nanophase ceramics [2].

Previous studies have shown that metal ions have a tendency to form ionic clusters in a polymer matrix and exist as microphases that are separated by the hydrophobic portions of the polymers [3]. These ionic domains that range in diameter between 2–10 nm are surrounded by the polymer network. The reduction of these dispersed metal ionic domains can result in ultrafine metal particles [4].

In this study it was found that nanometer sized crystalline Fe_3O_4 dispersed in a polymer matrix can be prepared by the oxidation of ultrafine iron powders in a polymer matrix under certain conditions.

2. Experimental procedures

2.1. Sample preparation

2.1.1. Matrix polymerization

The polymeric matrices used in this study were copolymers of vinylstyrene with 4-vinylpyridine (SVP) and poly(4-vinylpyridine) (PVP) that were synthesized by emulsion polymerization of redistilled styrene and 4-vinylpyridine, using potassium persulfate as an initiator (0.1–1 wt % of monomer) and sodium lauryl sulphate as a surfactant [5] (3 wt % of monomer). The precipitated products were filtered by suction and washed with water and then dried. The composition of the copolymers corresponding to the ratios of the two monomers is listed in Table I. The number-letter 11 and 51 in the sample code represent the mole ratio of vinylstyrene to 4-vinylpyridine (1:1, 5:1).

2.1.2. Preparation of the polymer–metal co-ordination complexes

The precursor polymers were dissolved in dimethylformamide (DMF) with stirring at 60 °C, and slowly mixed with a stoichoiometric amount of iron chloride hydrate ($FeCl_3 \cdot 6H_2O$) which was predissolved in DMF. After vigorously stirring and refluxing at 60 °C for about 1 h, the viscosity of the resulting solutions markedly increased which indicated the appearance of intermolecular crosslinking [3]. To prepare transparent thin films, the viscous solutions were cast into Teflon molding plates and dried for 24 h in an oven at 60 °C. Both SVP and PVP iron co-ordinated films were prepared.

2.1.3. Preparation of ultrafine metal particles

This SVP- or PVP-metal co-ordination films were dipped into a mixed solvent of DMF and water, which was then reduced by the dropwise addition of NH_2–NH_2 with stirring at room temperature for 1 h. The colour of the films quickly darkened and a large number of small bubbles were seen in the solution. The reduced films were thoroughly washed with water and dried in a vacuum oven at room temperature.

2.1.4. Preparation of ultrafine metal oxide particles

After the films were reduced by NH_2–NH_2, ultrafine particles of iron oxide were produced by oxidizing the

iron particles using NaOH. In this procedure aqueous NaOH was added dropwise to the solution to bring the pH to 13–14 and the resulting mixture was stirred for 2 h at 60 °C. The films were then washed with water to neutral pH and dried.

2.2. Analysis and characterization

Transmission electron microscopic (TEM) observations were performed using a drop of sample solution diluted in DMF ($\sim 0.01\ g\,ml^{-1}$) that was absorbed onto a carbon-coated grid. The micrographs were obtained on a Jeol, JEM-200 CK analytical electron microscope at an accelerating voltage of 200 kV. Electron spectroscopy for chemical analysis (ESCA) was performed on a VG Scientific Ltd mode LAB MK-II, apparatus using an argon ion beam to peel off the surface of the samples to allow analysis. The infra-red (IR) spectra were measured using a Nicolet 170SX FT-IR spectrometer. The X-ray diffraction (XRD) patterns of powdered samples were measured using a Rigaku D/MAX-RA diffractometer using CuK_α radiation generated at 40 kV and 150 mA. The magnetic hysteresis loop was measured using a vibrating sample magnetometer, while the magnetic susceptibility was measured on a Guoy balance.

3. Results and discussion

3.1. Fourier transform infrared measurements

The structures of polymer–metal coordination complexes have been studied by Agnew [6] and Grady *et al.* [7] on the basis of magnetic measurements and X-ray absorption patterns. The average co-ordination behaviour of polymer–metal chloride complexes obtained from solution is similar in a number of respects to that of monomeric vinylpyridine complexes. The pyridine groups replace waters of hydration and co-ordinate with the metal cation. These co-ordination bonds act as crosslinks that cause a corresponding strengthening of the material.

The co-ordination of the transition metal to pyridine is also observed in the IR spectra of the complexes [7, 10, 11]. As can be seen from Fig. 1 the bonds at 1671, 1555 and 1220 cm^{-1} can be attributed to $\nu_{C=C}$, $\nu_{C=N}$ and bending of PVP. Such bands appear at lower frequencies in spectra for complexes containing iron ions as a result of the co-ordination. The shift of aromatic carbon–nitrogen stretch absorption band to 1635 cm^{-1} after the addition of metal salts directly relates to the previously described specific interactions between the vinylpyridine and the transition-metal ions. Moreover, the band near 1635 cm^{-1} in the spectrum of PVP–Fe–R is much weaker than that of PVP–Fe, which suggests that the co-ordination in the former complex is not as strong as that in the latter one.

The IR spectrum of PVP–Fe–O is also shown in Fig. 1. The absorption band near 1635 cm^{-1} in the spectrum of PVP–Fe–O is also much weaker than that of PVP–Fe, showing that the co-ordination in PVP–Fe–O is weaker than that in PVP–Fe. The absorption bands on the trace of PVP–Fe–O at 893.3 and 400 cm^{-1} which are completely absent in the other three patterns are due to vibrations of the iron–oxygen bond.

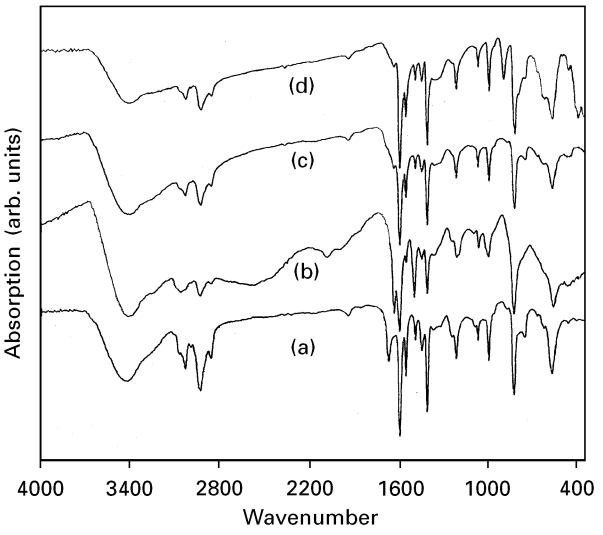

Figure 1 FT–IR absorption (a) PVP; (b) PVP–Fe; (c) PVP–Fe–R; (d) PVP–Fe–O.

TABLE I Composition of the samples

Sample	Polymer matrix	Ratio of vinylstyrene to 4-vinylpyridine	Products of the preparation step	Addition ratio of Fe^{3+} to pyridine
PVP–Fe	PVP	0	2.1.2	1:3
PVP–Fe–R	PVP	0	2.1.3	1:3
PVP–Fe–R–1	PVP	0	2.1.3	1:1
PVP–Fe–R–2	PVP	0	2.1.3	1:15
PVP–Fe–O	PVP	0	2.1.4	1:3
11–Fe	SVP	1	2.1.2	1:3
11–Fe–R	SVP	1	2.1.3	1:3
51–Fe	SVP	5	2.1.2	1:3
51–Fe–R	SVP	5	2.1.3	1:3

PVP: Poly(4-vinylpyridine)
SVP: styrene/4-vinylpyridine copolymer
S: vinylstyrene
4-VP: 4-vinylpyridine
R: Reduced sample
O: Oxidation sample

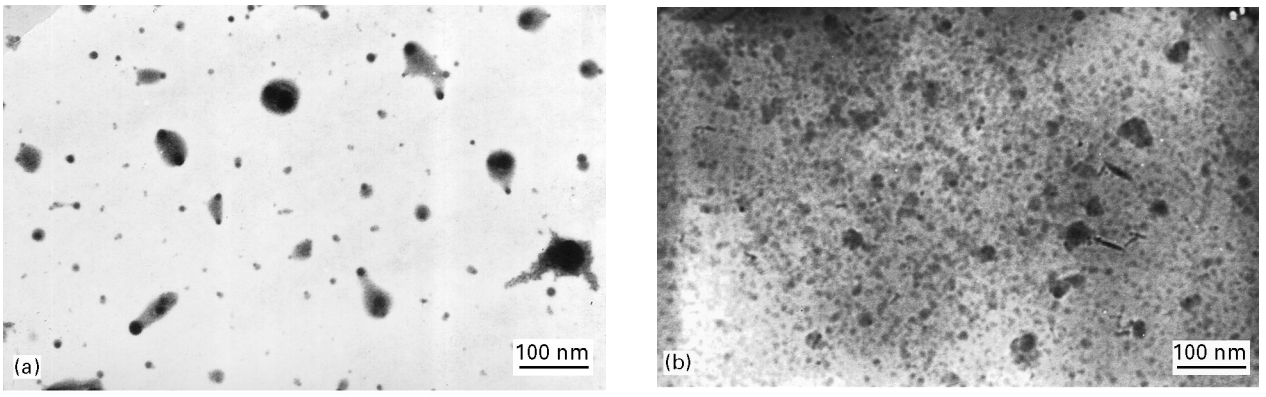

Figure 2 The morphology of the particles in polymer matrix (a) PVP–Fe–R and (b) PVP–Fe–O.

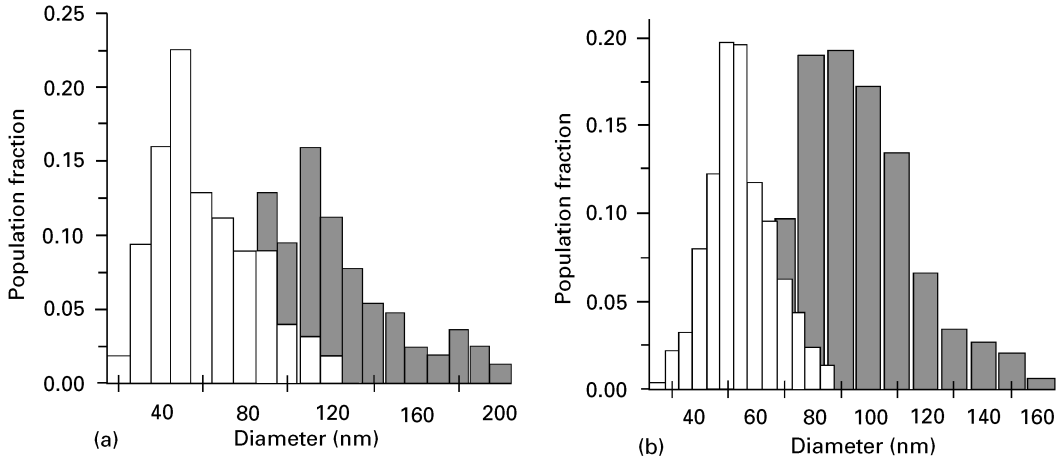

Figure 3 Size distribution of the ultrafine metal powders in the polymer matrix for (a) (■) SVP51–Fe–R and (□) PVP–Fe–R–2 and (b) (■) PVP–Fe–R–1 and (□) PVP–Fe–R.

3.2. Composition structure and size distribution of ultrafine metallic particles

TEM micrographs clearly indicated that the resulting ultrafine metallic particles were dispersed in the polymer matrix, as is shown in Fig. 2 (a and b). However, it was difficult to observed metal ionic aggregates in complexes before reduction using TEM because the interaction between the metal ions and the polymer ligands is strong and the ionic aggregates were too loose to form enough electron density contrast for observation. Therefore, the reduction step is indispensable to the preparation of ultrafine particles in this process.

The particles show a nearly spherical morphology with diameters ranging between 20–200 nm. The size distributions are given in Fig. 3 (a and b). The particle sizes were larger than expected due to cluster aggregation. According to a previous study [3], the clusters have a tendency to aggregate since this reduces the energy associated with the high surface area to volume ratio. However, by using the polymer matrix, the size of the ultrafine particles remains of nanoscale dimensions. Energy dispersive X-ray spectroscopy (EDX) has shown that these particles were composed of metallic atoms (characteristic peaks detectable in the corresponding metal element K_α energy position), as shown in Fig. 4. No distinct diffraction pattern revealing the existence of a crystalline phase could be seen.

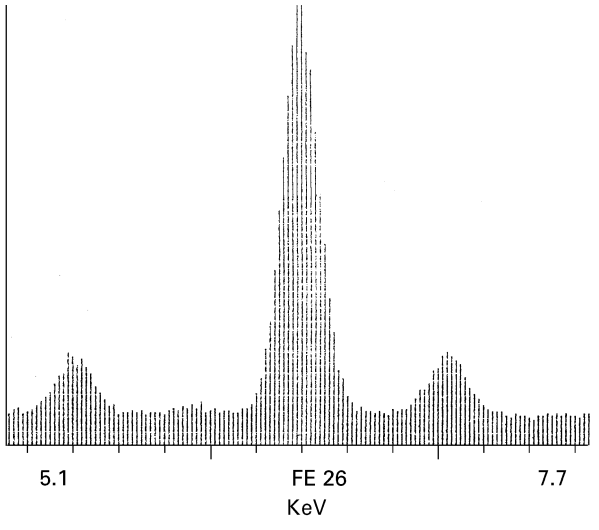

Figure 4 EDX pattern for SVP51–Fe–R.

In Fig. 3a, the effect of different base polymers on the size of the metallic particles is studied. The

diameter of the metal particles dispersed in PVP is smaller than those in SVP51 while the molar concentrations of metal ions of the two systems are the same since the pyridine groups could co-ordinate to the metal centre via σ-bonding which to a certain degree hinders the metal aggregation. In addition to the polarity of the polymer matrix, the concentration of the metal ions also has some effect on the size of the metal aggregates. As is shown in Fig. 3b, a higher concentration of metal ions causes larger particles.

A TEM micrograph of the sample film after oxidation is shown in Fig. 2b. The particles also show a nearly spherical morphology which is similar to the metallic iron powders.

3.3. ESCA analysis

In order to further analyse the chemical state of the ultrafine particles dispersed in the polymer matrix, the reduced complex film was investigated using the ESCA technique.

ESCA mainly deals with elemental composition (except for H, He) and the chemical state of the element in the material. Due to different atomic structures and chemical environments, the binding energies of electrons in inner shells of different atoms are characteristic. So with the elemental binding energies measured by ESCA, we can highlight particular features of peak envelopes and the composition of the exposed layers [9].

The ESCA spectrum of the reduced sample whose surface was peeled off with an argon ion beam is shown in Fig. 5. After correction for the electron shielding-effect the experimentally measured results of 710.6 and 712.0 eV become 708.5, the standard, and 709.9 eV, which indicate the existence of Fe(0) and Fe(II), respectively. The positive chemical shifts compared with the standard data suggest the co-ordination of iron to nitrogen. Since the electronegativity of N is greater than that of Fe, the negative charge density around an Fe atom co-ordinated to N decreases thereby diminishing the shielding-effect on electrons in the 2p orbital and strengthening the binding of these electrons to the nucleus. Therefore, the binding energy increases which leads to the positive chemical shift. The above analysis leads to the conclusion that after the reducing step, Fe^{3+} has been reduced to metallic Fe(0) and Fe(II), with some of the product also co-ordinated to nitrogen. The existence of Fe(II) is perhaps due to incomplete reduction or the oxidation of ultrafine metallic particles.

3.4. Wide angle X-ray diffraction analysis

In order to identify the crystal structure of the iron oxide that is present after the oxidation step, the powdered samples were examined by means of X-ray diffraction. The position (2θ) and intensity (I/I_0) of the scattering peaks are listed in Table II. Fig. 6 shows the X-ray diffraction patterns of the samples as a function of the diffraction angle (2θ). In the vicinity of 21°, the pattern for (a) PVP and (b) PVP–Fe–R exhibit halo peaks which are typical of amorphous substances. A weaker halo peak near 35° in (b) which is absent in (a) implies the existence of metallic iron aggregates. No sharp crystalline peaks can be seen in these two patterns, which is in agreement with the EDX results. However, significant differences are observed in the pattern for the PVP–Fe–O sample. Distinct sharp crystalline peaks appear with *d* values closely in accordance to those of a reference sample of magnetite Fe_3O_4, as shown in Table II, which indicates that the ultrafine particles obtained after oxidation of PVP–Fe–R are Fe_3O_4.

3.5. Magnetic property analysis

The magnetic properties of the ultrafine metal oxide particles are of great interest. Amongst all the metal oxide samples we measured on the vibrating-sample magnetometer, including 11–Fe–R, PVP–Fe and PVP–Fe–O, only PVP–Fe–O gave a detectable result, which is shown in Fig. 7. The magnetization hysteresis loop of PVP–Fe–O is typical for ferromagnetic and subferromagnetic materials [12]. The remanence B_R is defined as the magnetization remaining

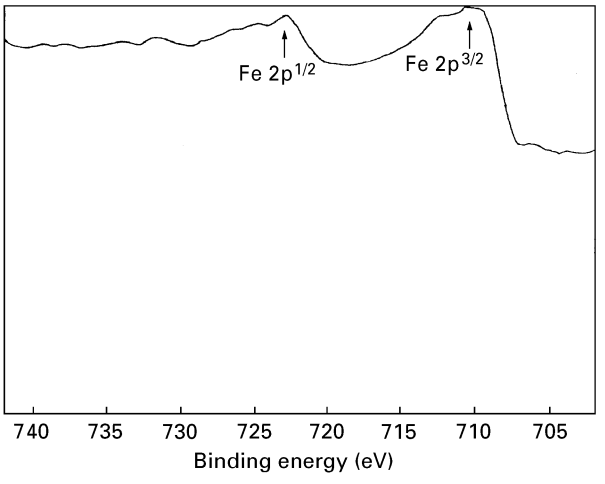

Figure 5 ESCA spectrum of PVP–Fe–R.

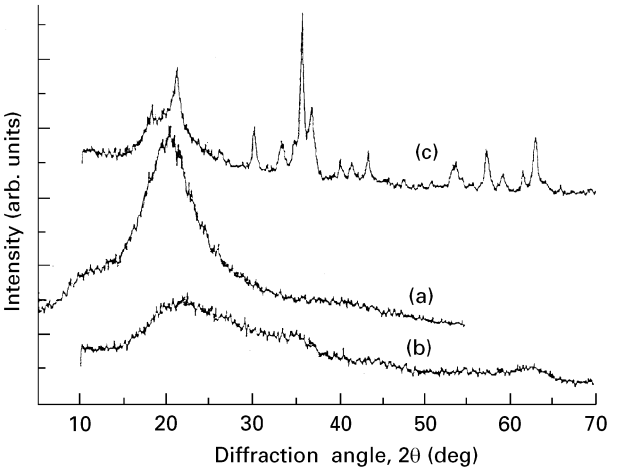

Figure 6 X-ray diffraction angle patterns of (a) PVP; (b) PVP–Fe–R and (c) PVP–Fe–O.

TABLE II Diffraction angles (2θ) and plane distances (d) corresponding to the peaks observed in the XRD pattern of the PVP–Fe–O powder sample

Peak		1	2	3	4	5
Diffraction angle (2θ)		30.040	35.391	43.065	53.443	62.597
PVP–Fe–O	d	2.971	2.534	2.098	1.713	1.482
experiment	I/I_0	39	100	27	20	25
Magnetite Fe_3O_4	d	2.967	2.532	2.099	1.715	1.484
Reference sample	I/I_0	30	100	20	10	40

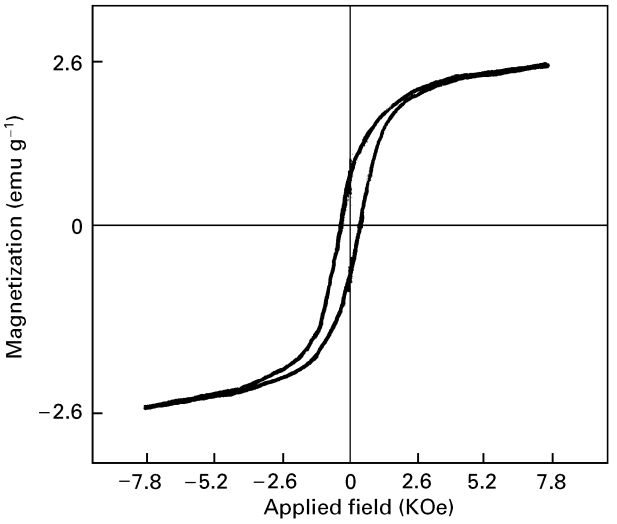

Figure 7 Magnetization hysteresis loop of PVP–Fe–O.

when the magnetic field is switched off from saturation, and the coercivity H_c is the reverse field required to reduce the magnetization to zero from saturation. The magnitude of H_c is influenced by the particle size and homogeneity of each material. The coercivity H_c of the synthesized PVP–Fe–O sample is 394 Oe. In this study, the magnetic material is heterogeneous, consisting of islands of a strongly magnetized phase embedded in a matrix of a weakly magnetized or non-ferromagnetic phase.

4. Conclusion

The compositional behaviour and morphology of metal-containing polymer materials were extensively studied by various measurement techniques in this paper. It was found that iron ions may co-ordinate to pyridine groups present in precursor polymers and thus form co-ordination polymers. The reduction of these dispersed metal ionic domains can result in ultrafine metal particles. The protective polymers play an important role in the preparation of the dispersions. Moreover, the co-ordination polymers have other potential advantages as a source of materials since the functional site concentration and consequently the size of the powders could be controlled. The oxidation of ultrafine iron particles in a polymer matrix results ultrafine magnetite Fe_3O_4 whose crystalline structure was confirmed by X-ray diffraction.

Acknowledgements

We would like to thank Zhu Yuping for the excellent experimental assistance during the X-ray diffraction experiments, Jian Zhensheng for his magnetic hysteresis loop works, and Hong Jianming for his help in performing the TEM observations.

References

1. R. BIRRINGER, U. HERR and H. GLEITER, *Trans. Jpn. Inst. Met.* **27** (1986) 43.
2. R. W. SIEGEL, S. RAMASAMY, H. HAHN, Z. LI, T. LU and R. GRONSKY, *J. Mater. Res.* **3** (1988) 1367.
3. A. EISENBERG and F. E. BAILEY, (eds) "Coulombic interactions in macromolecular systems" (ACS, Washington, DC, 1986).
4. L. CHEN, C. Z. YANG and X. H. YU, *Chinese Chem. Lett.* **5** (1994) 443.
5. P. K. AGARWALY, J. DUVDERVANI, D. G. PEIFFER and R. D. LUNDBERG, *J. Polym. Sci. B* **25** (1987) 839.
6. N. H. AGNEW, *J. Polym. Sci. Polym. Chem.* Ed. **14** (1976) 2819.
7. B. P. GRADY, E. M. O'CONNELL, C. Z. YANG and S. L. COOPER, *J. Polym. Sci. B.* **32** (1994) 2357.
8. D. J. CLOUTHIER and D. A. RAMSAY, *Ann. Rev. Phys. Chem.* **34** (1983) 31.
9. C. C. YEN and T. C. CHANG, *J. Appl. Polym. Sci.* **40** (1990) 53.
10. W. KÜNDIG and H. BÖMMEL, *Phys. Rev.* **142** (1966) 327.
11. D. G. PEIFFER, *et al.*, *J. Polym. Sci. Polym. Lett.* Ed **24** (1986) 581.
12. J. CRANGLE, in "The magnetic properties of solids" (Arnold, London, 1977).

Received 21 August 1995
and accepted 3 September 1996